

## A novel dual-LED based long-path DOAS instrument for the measurement of aromatic hydrocarbons



Jochen Stutz<sup>a,\*</sup>, Stephen C. Hurlock<sup>a</sup>, Santo F. Colosimo<sup>a</sup>, Catalina Tsai<sup>a</sup>, Ross Cheung<sup>a</sup>, James Festa<sup>a</sup>, Olga Pikelnaya<sup>a,1</sup>, Sergio Alvarez<sup>b</sup>, James H. Flynn<sup>b</sup>, Matthew H. Erickson<sup>b,c</sup>, Eduardo P. Olaguer<sup>c</sup>

<sup>a</sup> Department of Atmospheric and Oceanic Sciences, University of California Los Angeles, Los Angeles, CA 90095, USA

<sup>b</sup> University of Houston, Houston, TX, USA

<sup>c</sup> Houston Advanced Research Center, Houston, TX, USA

### HIGHLIGHTS

- A new instrument for fence-line monitoring of aromatic hydrocarbons was developed.
- A novel dual-LED light source improves LP-DOAS observations of aromatics.
- Accurate LP-DOAS observations of benzene, toluene and xylenes were demonstrated.
- Two-dimensional concentrations fields were determined using Tomographic LP-DOAS.

### ARTICLE INFO

#### Article history:

Received 9 May 2016

Received in revised form

23 August 2016

Accepted 22 September 2016

Available online 28 September 2016

#### Keywords:

Benzene

Toluene

Differential optical absorption spectroscopy

Computer aided tomography

Emissions

### ABSTRACT

Aromatic hydrocarbons are well known air toxics which are regulated by the US EPA and other air quality agencies. Accurate, long-term monitoring of these compounds at low part-per-billion levels, as well as identifying emission point sources is therefore crucial to protect human health in neighborhoods near large emission sources. Here we present a new long-path differential optical absorption spectroscopy (LP-DOAS) instrument specifically designed to monitor aromatic hydrocarbons. The system is based on a novel dual - light emitting diode (LED) light source, which eliminates the requirement to suppress spectrometer stray light. This light source, together with a high stability fiber-based sending/receiving telescope, allows the measurement of aromatic hydrocarbons on once-folded absorptions paths of 200–1200 m length. The new instrument shows very good agreement with simultaneous in-situ measurements if inhomogeneities of the trace gas spatial distributions are considered. The new instrument performed well during a three-month field test as an automated fence-line monitor at a refinery, successfully distinguishing upwind background levels of ~1 ppb from emissions reflected in elevated mixing ratios of 3–4 ppb. A two-dimensional measurement network based on two identical LP-DOAS instruments operating on seven crossed light paths was operated successfully in Houston, TX. Qualitative and quantitative analysis of two events with toluene and xylene plumes demonstrate how this setup can be used to derive the spatial distribution of aromatic hydrocarbons, and identify point sources.

© 2016 Elsevier Ltd. All rights reserved.

### 1. Introduction

Long Path Differential Optical Absorption Spectroscopy (LP-DOAS) is a powerful method for identifying and quantifying

pollutants in the UV/visible spectral region using their unique narrow-band absorption features (Platt and Stutz, 2008). LP-DOAS has been a staple of atmospheric chemistry research for several decades, but its implementation for air quality monitoring has been slow, and only moderately successful. The most common use of LP-DOAS has been the monitoring of pollutants such as O<sub>3</sub>, SO<sub>2</sub>, and NO<sub>2</sub>, as well as research of the chemistry of HCHO, HONO, NO<sub>3</sub>, halogen oxides, glyoxal, and other short-lived reactive species (Platt and Stutz, 2008).

\* Corresponding author.

E-mail address: [jochen@atmos.ucla.edu](mailto:jochen@atmos.ucla.edu) (J. Stutz).

<sup>1</sup> Now at South Coast Air Quality Management District, Diamond Bar, CA, USA.

Another class of compounds that can be measured by LP-DOAS is aromatic hydrocarbons, such as benzene, toluene, xylenes (BTX), etc. (Axelsson et al., 1995; Barrefors, 1996; Skov, 2001; Trost et al., 1997; Volkamer et al., 1998; Wideqvist et al., 2003). Aromatic hydrocarbons are known for their various detrimental health effects (Snyder et al., 1993; Weisel, 2010). Benzene is a known carcinogen for which the US EPA and WHO do not define a safe lower limit of exposure (<http://www.epa.gov/airtoxics/hlthef/benzene.html>, [http://www.who.int/ipcs/assessment/public\\_health/benzene/en/](http://www.who.int/ipcs/assessment/public_health/benzene/en/)), while the evidence for carcinogenicity is inconclusive for toluene and xylenes (<http://www.epa.gov/airtoxics/hlthef/toluene.html>, <http://www.epa.gov/airtoxics/hlthef/xylenes.html>). Aromatics also contribute to the formation of secondary pollutants such as ozone and particles in urban areas (Finlayson-Pitts and Pitts, 1999). Sources of aromatics include vehicles, solvent use, and the petrochemical industry. The latter has received considerable attention due to high BTX levels in neighborhoods adjacent to petrochemical facilities, and recent accidents leading to enhanced releases of these compounds. The US EPA recently adopted a rule on “Petroleum Refinery Sector Risk and Technology Review and New Source Performance Standards” (<http://www.epa.gov/airtoxics/petref.html>), which, for the first time, defines a requirement for refineries to monitor fence-line benzene concentrations, and establishes a 2-week averaged benzene concentration action level of ~3 ppb. Consequently, there has been a push to better monitor the release of BTX from petrochemical facilities on long time scales. In addition, there is a need for a rapid alarm system to warn neighbors of accidental releases.

LP-DOAS offers a unique opportunity to address these current needs, and it is thus somewhat surprising that it has not found more widespread use as a fence-line and neighborhood-scale monitor for aromatic hydrocarbons. This may be, in part, due to the lack of reliable, easy-to-use LP-DOAS instruments to measure aromatics, as well as a number of difficulties in the application of LP-DOAS for these observations. DOAS is a well-established method to measure path-integrated trace gas absorptions and concentrations in the open atmosphere (Platt and Stutz, 2008). The basis of DOAS is the identification and quantification of narrow-band absorptions in the UV–vis wavelength range along an open absorption path in the atmosphere using the Beer–Lambert law and well-known trace gas absorption cross sections. The measurement in the open atmosphere, together with the fact that the absorption cross sections are intrinsic physical properties, makes DOAS an absolute analytical technique that does not require calibration. LP-DOAS instruments typically consist of a light source, a telescope and reflector (monostatic setup) or sending and receiving telescopes (bistatic setup) that define the atmospheric absorption paths, and a spectrometer/detector combination to record the absorption spectra.

Despite the advantages of LP-DOAS and its potential to serve as long-term monitors for BTX, it has not found widespread use either in commercial or research applications. A few commercial instruments are currently available (for example from OPSIS Inc.), which have also been used for research applications. Research grade instruments are even more sparse. These systems are all based on general purpose LP-DOAS instruments and use Xe arc lamps, which emit light in a broad spectrum from the UV to the near IR, as light sources. Both monostatic and bistatic telescope setups have been used. However, most research grade instruments have been based on a combination of a coaxial Newtonian sending and receiving telescope on one end of the light path, and an array of corner cube retroreflectors on the other end.

The use of Xe-arc lamps brings with it a number of challenges. The absorption of BTX occurs in a spectral interval between 250 and 290 nm. A Xe-arc lamp only emits ~1.5% of its power below the

typical detector cut-off of ~1000 nm in this range. This value is further reduced, often well below 1%, when light is transmitted over long paths in the atmosphere, as oxygen and ozone absorption and Rayleigh scattering further reduce the intensity in the BTX wavelength range relative to higher wavelengths. Incomplete suppression of light outside the BTX range leads to stray-light in the spectrometer (Platt and Stutz, 2008), which can severely impact the performance of an LP-DOAS. Little quantitative information on straylight levels in the BTX range are available, but previous unpublished experiments found straylight levels that can reach 10% or higher. It should be noted that this problem becomes more severe with increasing absorption path-length, and often determines the longest path-length that can be achieved. Some studies have used additional filters to address this problem (Lee et al., 2005; Platt and Stutz, 2008; Trost et al., 1997; Volkamer et al., 1998), but in many cases, and in particular with some of the commercial systems, it is unclear how this effect impacts performance. As we will describe below, one solution for this problem is the use of newly available deep-UV light emitting diodes (LED), which emit light only in the desired wavelength range. LED's have other advantages compared to Xe-arc lamps, such as a long lifetime and low power consumption.

A second major challenge in using LP-DOAS to measure BTX is the presence of strong, and often saturated, overlapping absorptions of oxygen and oxygen collisional complexes. The accurate description of these structures is crucial for a successful DOAS analysis (Peng et al., 2008; Volkamer et al., 1998). Commercial systems, and sometimes also research grade instruments, thus use an atmospheric reference spectrum, measured on the same light path during times of low BTX levels. The obvious challenge here is the identification of such times, and in reality the BTX measurements can only be considered relative to this reference spectrum. This approach is also unsuitable to correct for the oxygen concentration changes due to atmospheric temperature and pressure variations. Because the shape of the oxygen absorption structures strongly depends on the pathlength, every light path would also require its own reference spectrum, potentially leading to concentration biases among different light paths.

The use of new technology, such as LEDs, could also aid in improving and expanding the practical capabilities of LP-DOAS BTX systems. LED's have much better long-term stabilities than Xe-arc lamps, and it should thus be possible to design stable instruments that can make unattended measurements over long time periods, months to years, thus reducing the operational cost of fence-line measurements. Previous instruments also did not explore the capability to measure on more than one light path, thus covering an extended area with observations, or, as discussed below, use two instruments to allow 2D concentration field retrievals.

The performance of currently available LP-DOAS instruments is also not well understood. Comparison of commercial LP-DOAS instruments to other observational methods have shown them to be inconsistent (Barrefors, 1996; Kim, 2004; Villanueva et al., 2012; Xie et al., 2004). The comparison with research grade instruments is generally better (Jobson et al., 2010; Kim and Kim, 2001; Peng et al., 2008), with some differences commonly attributed to spatial differences between the in-situ techniques and the LP-DOAS setup.

To address the challenges and opportunities with LP-DOAS instruments to measure aromatic hydrocarbons, we have developed the next generation of instruments that overcome some of the problems listed above. Here we describe the new LP-DOAS system and the analysis method to retrieve path-averaged mixing ratios. Data from deployments as a fence-line monitor and as a novel setup with two LP-DOAS instruments operating on multiple crossed

lights path in Houston, TX, will be presented. In addition, the new LP-DOAS was compared to in-situ measurements during the Benzene and other Toxics Exposure (BEE-TEX) field experiment in Houston, TX in Winter 2015. This comparison gives insight into its performance on single and multiple light paths. We will briefly present the results of the retrieval of 2D mixing ratio distributions from the LP-DOAS observation. A more detailed discussion on the retrieval methodology and a discussion of these results is presented in the companion paper by Olaguer et al.

## 2. Instrument description

Our new LP-DOAS BTX instrument is a monostatic setup, i.e. a combined sending/receiving telescope and a retroreflector array (Fig. 1, S1 and Table 1). The main part of the instrument consists of a new deep-UV LED based light source, a spectrometer-detector combination, a coaxial sending/receiving telescope, and a bifurcated quartz fiber bundle (Fig. 1). These components will be described in the following section, and are also summarized in Table 1.

### 2.1. LED light source

Motivated by the desire to eliminate spectrometer straylight from wavelengths above 290 nm, which is common for previous LP-DOAS BTX instruments that use Xe-arc lamps, and to develop a more stable and long-lived light source, we used novel UV Light Emitting Diodes (LEDs) as our light sources in the 250–290 nm region. These LEDs are commercially available at center wavelengths at 10 nm intervals with 10–15 nm wide emission intervals (Sensor Technology Inc., UCTOP Deep UV LED with ball lens). In comparison to classic Xe-Arc lamps, the LED's have several advantages. Their lifetime is in the range of 3000–10000 h (exact information on our LEDs is not available. The lower limit is based on our direct observations), and is thus longer than that the typical Xe-arc lamp lifetime of 200–2000 h (Platt and Stutz, 2008). Their power consumption is 0.5–1 W, much smaller than other light sources. The optical output varies from LED to LED but is generally in the range of 3  $\mu\text{W}/\text{nm}$  for a 250 nm LED and 8  $\mu\text{W}/\text{nm}$  for a 265 nm LED. Assuming an f/4 optical setup, this is comparable to that of a typical 150 W Xe lamp (Platt and Stutz, 2008).

Initial laboratory tests (not shown here) showed that the LEDs had excellent temporal stability and fairly smooth emission spectra, in contrast to the observations by Sihler et al. (2009) who found

substantial spectral structures in their UV LED, and were thus suitable for the use in LP-DOAS instruments. However, the small wavelength emission interval of the LEDs limits the LP-DOAS measurement to a subset of aromatic hydrocarbons. It is therefore necessary to use at least two LED's with different peak wavelengths to measure all BTX compounds. To avoid the complexity of a mechanical system to switch LEDs and to allow for simultaneous measurement of all BTX compounds, we developed an optical fiber setup that combines LEDs for two different wavelength intervals to expand the useable wavelength range. Combining the output of two LEDs has to be done with care, as relative variation of the combined signals, due to drift and noise in the LED power supply, aging of the LEDs and optical components, and variations of LED output with temperature, could introduce unwanted differential structures in the atmospheric absorption spectra, and thus interfere with the DOAS analysis. In addition, problems may arise if the outputs of the two LEDs are imperfectly aligned with each other, or if they have an uneven distribution of the LED output over the open aperture of the light beam. This may lead to slightly different light paths through the atmosphere for each LED output, due to turbulence or other atmospheric effects, which may cause temporal variations of the relative intensities of the two LEDs, and thus also change the shape of the observed combined spectrum.

The fiber-based optical combiner/mixer described here gives a uniform light beam of the two combined LED outputs, which provides a uniform dual LED light source that is temporally stable and easy to use. First, each LED is carefully aligned with the input of a 660  $\mu\text{m}$  diameter quartz fiber bundle, consisting of seven 200  $\mu\text{m}$  quartz fibers (Fig. 1). The diameter of this bundle end was chosen to allow collection of a significant amount of the LED light at the focus of the LED lens, which we measured to be approximately 0.8–1 mm in diameter. Each bundle end was placed in an x-y optical alignment mount and its position was optimized for maximum intensity. It should be noted that the LEDs were delivered with a ball lens that projects a focus of the emitted light at  $\sim 15$  mm distance. This setup is thus quite small and compact. The fibers from the two 660  $\mu\text{m}$  bundles were combined into one  $\sim 1$  mm diameter bundle (Fig. 1). This bundle end was then connected to a single 1 mm diameter, 1 m long, fiber that ensured that the outputs of the two LEDs were mixed. The 1 mm diameter fiber end was used as the light source in the LP-DOAS system. The spectral structure of this setup (Fig. 2) shows that a useable wavelength range from  $\sim 252$  to 280 nm can be achieved by combining 260 nm and 270 nm LEDs. This range includes all the absorptions of BTX and other aromatic hydrocarbons

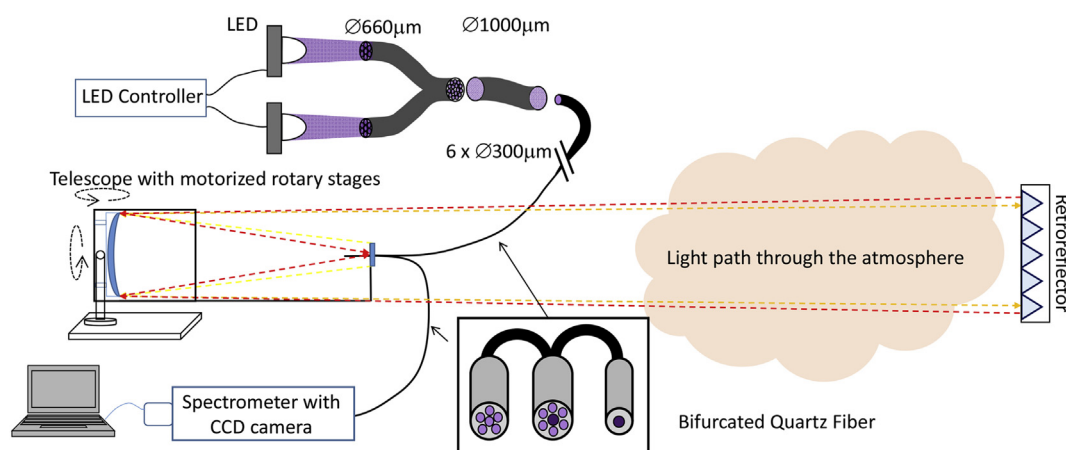


**Fig. 1.** Sketch of the new UCLA Mini LP DOAS instrumental setup. The insert shows the ends of the bifurcated fiber – common end to the telescope, the fiber bundle to the light source, and receiving fiber to the spectrometer.

**Table 1**  
Details of the setup of the new LP-DOAS system.

Sending/receiving telescope	Homebuilt telescope based on 120 cm focal length, 12 inch diameter spherical main mirror with aluminum coating. Rotation capability in azimuth and elevation using two high accuracy rotational stages (Newark systems RT-5 rotational stages with Arcus Inc. USB integrated stepper motor). Automated short-cut system to measure LED emission spectrum using stepper motor controlled by Arcus Inc. PMX-2ED controller.
Optical fibers	A combination of three silica-silica fibers connects light source, telescope and spectrometer: <ul style="list-style-type: none"> <li>• Bifurcated fiber bundle with total <math>2 \times 7 = 14</math> 200 <math>\mu\text{m}</math> <math>\varnothing</math> fibers, length 2.5 m</li> <li>• Single <math>\varnothing = 1</math> mm, length 1 m</li> <li>• Bifurcated fiber bundle with total <math>1 + 6 = 7</math> 300 <math>\mu\text{m}</math> <math>\varnothing</math> fibers, length 5 m</li> </ul>
Spectrometer	Acton 300 grating spectrometer, using 1800 g/mm holographic grating covering 50 nm range, with spectral resolution of $\sim 0.3$ nm. Thermally stabilized to 35 °C
Detector	Princeton Instrument, PIXIS 256 CCD detector, with E2V UV-enhanced back-thinned 1024 $\times$ 256 CCD.
Light source	Combination of 255 nm and 265 nm UV LED with ball lens (see text for details) powered by Mightex high precision LED driver.
Reflector	Solid quartz corner cube reflector array. Diameter of individual reflectors 57 mm. Number of reflectors varies from 10 to 25 depending on path length
Alignment aids	- Fully automated alignment capability, using UV LED intensity and detector. - Camera to aid in alignment of telescope and to remotely check visibility
Computer/software	Industrial personal computer running DOASIS (Univ. Heidelberg).

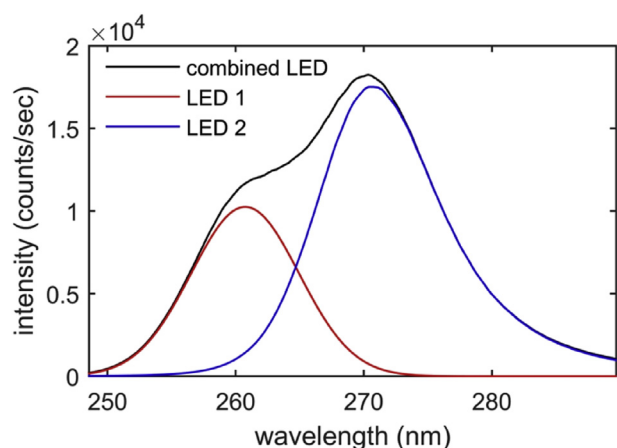


**Fig. 2.** Emission spectrum of the dual LED setup during the field experiment in Houston, TX, (black line). The red and blue line show the emission spectra of the individual LED's. (For interpretation of the references to colour in this figure legend, the reader is referred to the web version of this article.)

(Fig. S2). The transmissivity of the setup is predominantly determined by the geometric loss of combining fibers with different geometries, with a smaller contribution of the transmissivity of the fiber ends. Overall, the transmissivity from one LED to the output of the 1 mm fiber is  $\sim 7\%$ . It is difficult to compare this loss with other possible setups, as the optical combination of the two LED's would require a more complex optical setup, including beam splitters and various lenses/mirrors, to achieve a similar level of optical mixing between the two LEDs.

## 2.2. Telescope

The new LP-DOAS telescope is based on a design described by (Merten et al., 2011), which uses a fiber bundle instead of the secondary mirrors in a coaxial Newtonian sending/receiving telescope. The fiber bundle consists of a 300  $\mu\text{m}$  diameter fiber surrounded by six 300  $\mu\text{m}$  diameter fibers. The six fibers are used to transfer the light from the LEDs to the telescope, while the single fiber is used to receive the light that is returned from the retroreflectors. This design has several advantages over a classical Newtonian coaxial arrangement (Merten et al., 2011). The optical setup is much simpler, thus allowing a higher throughput than in classical Newtonian telescopes, in particular in the UV where high mirror reflectivities are difficult to achieve at a reasonable cost. The simplicity of the setup also improves the stability of the telescope

and its internal alignment. The telescope was pre-aligned for a collimated outgoing light beam in the laboratory. The fiber position was then adjusted in the field for optimal light return, typically by moving it 1–2 mm out of focus. In the case of multiple light paths, this alignment was made on the longest light path.

The telescope is mounted on a gimbal comprising two computer-controlled rotational stages, which allows rotation of the telescope by  $\sim 20^\circ$  in elevation and  $270^\circ$  in the azimuth. This capability serves two purposes. First, atmospheric refraction changes the alignment of an LP-DOAS setup throughout the day, which is compensated by an active control of the telescope aim. Second, the rotational stages allow sequential aiming at different retroreflectors. Consequently, one LP-DOAS system can measure on several light paths, a property which is required for vertical profiling and 2D concentration mapping. A third stepper motor was used to rotate a reflective diffuser (220 Grit glass substrate coated with UV-enhanced aluminum) in front of the bifurcated fiber in the telescope to regularly measure the emission spectrum of the two LEDs. We will refer to these measurements as LED spectra in the remainder of the manuscript.

The telescope was designed for outdoor deployment, i.e. it is equipped with a cover to protect the main mirror and motors from rain and snow, and for complete remote control through addition of a CCD camera with telescopic lens, which serves as an "aiming scope". This scope is calibrated carefully at the beginning of each deployment because, in contrast to LP-DOAS applications with a visible light beam, the reflection from the retroreflectors cannot be seen in our system.

## 2.3. Spectrometer-detector/electronics

A commercial spectrometer-detector system is used in the new LP-DOAS system. The spectrometer is a 300 mm focal length Czerny Turner instrument (Acton 2300) with a spectral resolution of 0.35 nm. To ensure long-term stability the spectrometer is thermally stabilized through heaters and a high accuracy temperature controller. It should be noted that high thermal stability has been found to be crucial for the performance of DOAS instruments (Platt and Stutz, 2008). The detector (Princeton Instrument PIXIS) is based on a 1024  $\times$  256 pixel back-thinned CCD detector, which was cooled to  $-70$  °C. Because the LED light source only emits light in the wavelength range in which aromatic hydrocarbons absorb, spectrometer stray light from other wavelengths is absent in our setup and no further measures have to be taken to reduce spectrometer stray light. It should be noted that the usual methods to determine spectrometer stray light, i.e. emitting light outside the observed wavelength range, does not apply here. We thus estimate

the spectrometer stray light based on previous experience with this type of spectrometers to be below 1% (Stutz and Platt, 1997).

The instrument is controlled by an industrial PC running the DOASIS software package (University of Heidelberg). The software is set up for fully automated operation on multiple user-selectable reflector locations. DOASIS controls the camera exposure, telescope alignment, and data storage on a local hard drive as well as on a cloud storage service. The measurement routine is specifically set up to the respective field deployment. For example, for a fenceline monitoring application atmospheric measurements are performed every minute, the telescope is re-aimed every 3 h to optimize the return intensity, and the spectrum of the LED is measured every 6 h. For the 2D application, the telescope is rotated onto a reflector, followed by an intensity optimization. A measurement is then performed for a total of 5 min, before aiming at another reflector. This sequence is only interrupted for measurements of the LED every 6 h. For all measurements the integration times are selected so that the detector saturation is around 50% and single observations are co-added for the desired measurement time.

### 3. Data analysis

The LP-DOAS instrument measures absorption spectra in the open atmosphere along an extended light path. To derive the path-averaged concentrations, a spectral retrieval that separates and quantifies the various overlying absorption structures using a linear combination of absorption cross sections reduced to the instrument resolution and a least squares fit is typically used. This approach, which has been successful in LP-DOAS observations of pollutants and other trace gases, has to be adjusted when working in the 250–290 nm range, due to the strong and highly structured molecular oxygen absorptions. In addition, the presence of  $O_2 \cdot O_2$  and  $O_2 \cdot N_2$  absorptions has posed a challenge in the past, as absorption cross sections for these collisional complexes have only recently become available (Fally et al., 2000). The most common way to perform an aromatics analysis of LP-DOAS observations is to use an atmospheric reference spectrum, i.e. a spectrum measured over the same light path at a time of low aromatic hydrocarbon concentrations. This analysis approach yields concentrations relative to the trace gas absorptions in the reference spectrum, which is problematic in areas where high background BTX levels are present, or when it is difficult to find a time period with low concentrations. Because our instrument is deployed in urban areas near petrochemical facilities, the atmospheric reference spectrum approach is thus not suitable. We have therefore pursued a strategy which relies on a purely mathematical retrieval of absorptions in a single atmospheric spectrum, which yields absolute BTX concentrations.

In typical LP-DOAS application, trace gas reference spectra are calculated by a convolution of a high-resolution absorption cross section with the instrument function using a smooth, or even constant, light source intensity spectrum  $I_0(\lambda)$  (Platt and Stutz, 2008). The instrument function is typically determined by measuring an atomic emission line, in our case from a mercury discharge lamp. The presence of the oxygen absorption structures (Fig. S1) in the 250–290 nm wavelength range, however, requires special consideration for the calculation of trace gas references for the BTX analysis, as the narrow  $O_2$  absorption bands are strong or even at saturation, even at fairly short light paths. Because typical DOAS instruments have spectral resolutions in the range of a few tenths of nanometers, the oxygen absorption structure is not resolved in the observations. This leads to a non-linearity of the dependence of oxygen absorption on the path length and concentration, which impacts the shape of the other trace gas absorptions in the analysis.

We have thus developed a new method to calculate trace gas

references in the 250–290 nm wavelength range, using the fact that the atmospheric oxygen mixing ratio is constant and that the concentration only varies by 10–20% due to pressure and temperature changes. As derived in the Supplement, the oxygen absorption spectral structure can be included in the light source spectrum used in the trace gas reference convolution (see supplement for the mathematical equations of this calculation). Thus the calculation of the trace gas reference spectra can be performed with a method that is commonly used for reference spectra calculation for sunlight absorption spectra, the so-called I0-effect (Platt and Stutz, 2008). To our knowledge this approach has not been previously used in LP-DOAS BTX measurements. A consequence of this approach is that trace gas reference spectra have to be calculated for each specific absorption path length and, in the case of multi-path observations, each path has its own set of references.

The high resolution absorption cross sections for  $O_2$ ,  $O_2 \cdot O_2$  and  $O_2 \cdot N_2$  used in the calculations of reference spectra were taken from (Fally et al., 2000), the ozone absorption cross section is from (Voigt et al., 2001), and the absorption cross sections for the aromatic hydrocarbons are from (Fally et al., 2009). Two oxygen reference spectra are calculated for two different concentrations, i.e. the second spectrum has a 20% lower  $O_2$  column density. The second spectrum is orthogonalized to the first and describes possible nonlinearities in the  $O_2$  absorption due to small changes in atmospheric oxygen concentrations. It should be noted that oxygen absorption reference spectra are calculated using a simple convolution of the absorption cross section, i.e. without the I0 effect.  $O_2 \cdot O_2$  and  $O_2 \cdot N_2$  absorptions are treated as normal trace gas absorption spectra, as their absorptions are much weaker and spectrally broad.

The atmospheric absorption spectrum, after division by the LED spectrum, and the reference spectra were smoothed to filter frequencies higher than expected from the spectrometer resolution.

The spectral retrievals were performed using a combination of a linear and non-linear least squares fit that fits a model function,  $F(\lambda)$ , consisting of a linear combination of the reference spectra and a polynomial of order  $n$  to the logarithm of the atmospheric spectrum divided by the LED spectrum.

The least squares analysis was performed on two separate wavelength intervals; one for benzene and one for toluene and the xylenes (Table 2). The benzene range covered the wavelength interval from 252 to 261 nm, while toluene and xylenes were analyzed in the wavelength interval from 263 to 274 nm, excluding a small interval from 265 to 266 nm due to a recurring unexplained structure which led to instabilities in the retrieval. Table 2 lists the reference spectra included in the fit, as well as the degree of the polynomial fitted to describe broadband absorptions (Platt and Stutz, 2008). In both windows the oxygen containing species were allowed a common small spectral shift of less than  $\pm 2$  pixel. Ozone and the respective aromatics were also allowed a small common spectral shift of  $\pm 2$  pixel. This shift allowed for the correction of temperature changes of the spectrometer, which in our Texas deployment was not constant. The statistical uncertainty of the trace gas mixing ratios is calculated by the fitting procedure for each spectrum using the methods described in Platt and Stutz (2008). This statistical error was multiplied by a factor of two to compensate for the smoothing applied to the spectra, roughly following the argument by Stutz and Platt (1997). The accuracy of the reported mixing ratios is dominated by the accuracies of the absorption cross sections, i.e. 5–15% for  $O_2$ ,  $O_2 \cdot O_2$  and  $O_2 \cdot N_2$  (Fally et al., 2000), 5% for ozone (Voigt et al., 2001), and <8% for benzene, toluene, p-xylene, and m-xylene (Fally et al., 2009). Accuracies of absorption path length, spectrometer stray light, and other instrumental effects are below 2%.

Fig. 3 shows an example of the spectral retrieval of benzene on

**Table 2**  
Details of the Manchester St. site LP-DOAS data analysis and detection limits under optimal conditions during BEE-TEX.

Species	Wavelength range	Trace gases fitted	Detection limit under optimal conditions, ppb M1 (770 m)/M2 (1203 m)/M3 (270 m)
Benzene	252–261 nm	O <sub>2</sub> , O <sub>3</sub> , O <sub>2</sub> ·O <sub>2</sub> , O <sub>2</sub> ·N <sub>2</sub> , benzene, polynomial degree 4	0.56/0.34/1.2
Toluene	263–274 nm excluding 265–266 nm	O <sub>2</sub> , O <sub>3</sub> , O <sub>2</sub> ·O <sub>2</sub> , O <sub>2</sub> ·N <sub>2</sub> , toluene, m-xylene, p-xylene, and polynomial degree 5	0.60/0.45/1.28
m-Xylene	263–274 nm excluding 265–266 nm	O <sub>2</sub> , O <sub>3</sub> , O <sub>2</sub> ·O <sub>2</sub> , O <sub>2</sub> ·N <sub>2</sub> , toluene, m-xylene, p-xylene, and polynomial degree 5	0.58/0.38/1.11
p-Xylene	263–274 nm excluding 265–266 nm	O <sub>2</sub> , O <sub>3</sub> , O <sub>2</sub> ·O <sub>2</sub> , O <sub>2</sub> ·N <sub>2</sub> , toluene, m-xylene, p-xylene, and polynomial degree 5	0.36/0.28/0.76

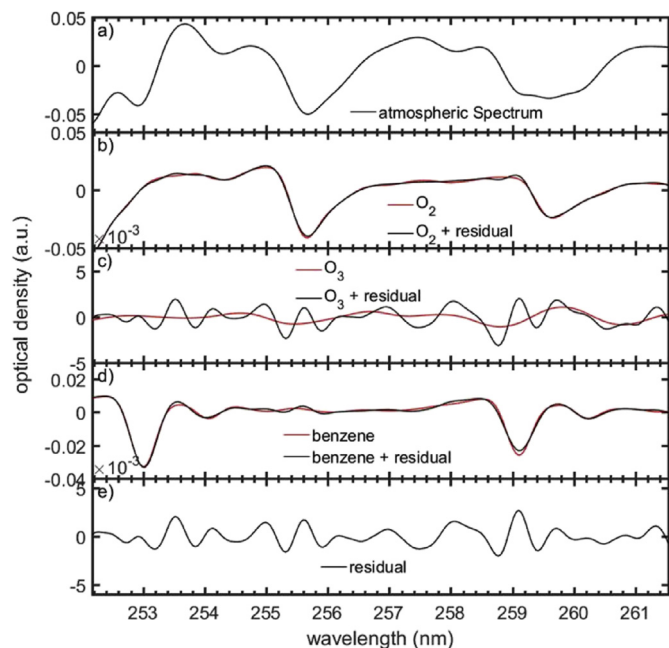


**Fig. 3.** Example of the spectral retrieval of benzene on 2/13/15 6:43 CST on the 270 m light path at the Manchester St. site. The red curves show the fitted reference spectra of the respective absorbers. The black curves are the fitted references with the unexplained residual structures of the retrieval added. The comparison of the two curves shows the clear identification of  $33 \pm 0.9$  ppb of benzene. (For interpretation of the references to colour in this figure legend, the reader is referred to the web version of this article.)

2/13/15 6:43 CST on a 270 m light path at the Manchester St. site in Houston. The comparison of the retrieved benzene absorption with the scaled reference spectrum shows the clear identification of  $33 \pm 0.9$  ppb of benzene. The residual of the fit is mainly determined by the photon noise in the spectrum. Fig. 4 shows the spectral retrieval of toluene and m-/p-xylene on 2/18/15 1:07 CST on the 770 m light path (M1) at the Manchester St. site. Toluene and the xylenes were clearly identified, with  $31.4 \pm 0.8$  ppb of toluene,  $11.0 \pm 0.6$  ppb of m-xylene, and  $4.9 \pm 0.2$  ppb of p-xylene.

The detection limits, reported here as twice the statistical mixing ratio error determined by the fitting procedure, as determined in the field from the average statistical error of the DOAS spectral analysis, are listed in Table 2. For all four aromatic hydrocarbons the detection limits are around 1 ppb or below. It should be noted that the common approach of listing detection limits for LP-DOAS system, i.e. minimal mixing ratios detectable on a specific light path, is not ideal in the case of inhomogeneously distributed gases, such as plumes along a fence line. A better quantity to report the detection limits is the trace gas column detection limit, i.e. the product of the mixing ratio detection limit multiplied by the path

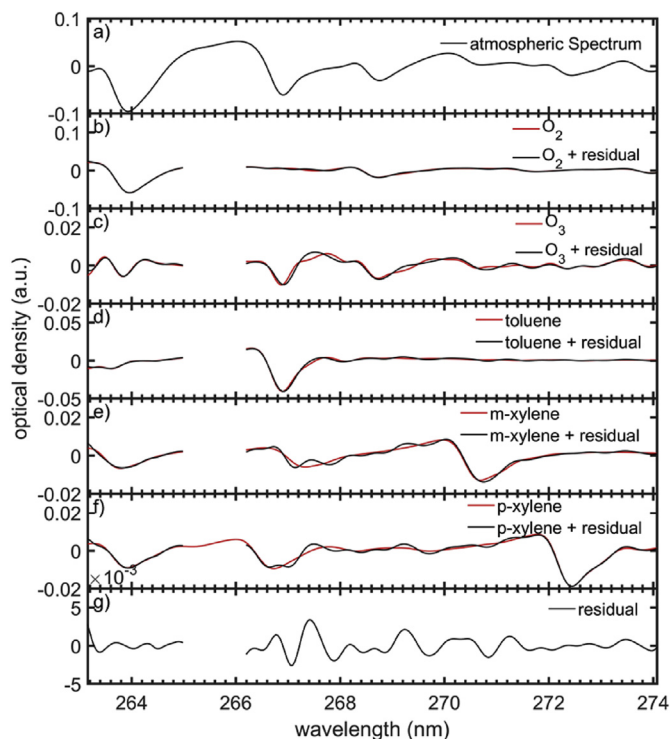


**Fig. 4.** Example of the spectral retrieval of toluene and m-/p-xylene on 2/18/15 1:07 CST on the 770 m light path (M1) at the Manchester St. site. The red curves show the fitted reference spectra of the respective absorbers. The black curves are the fitted references with the unexplained residual structures of the retrieval added. The comparison of the two curves shows the clear identification of  $31.4 \pm 0.8$  ppb of toluene,  $11.0 \pm 0.6$  ppb of m-xylene, and  $4.9 \pm 0.2$  ppb of p-xylene. (For interpretation of the references to colour in this figure legend, the reader is referred to the web version of this article.)

length. The column detection limit averaged for our 770 m and 1203 m long paths are:  $420 \text{ ppb} \times \text{m}$  for benzene,  $500 \text{ ppb} \times \text{m}$  for toluene,  $451 \text{ ppb} \times \text{m}$  for m-xylene, and  $307 \text{ ppb} \times \text{m}$  for p-xylene. It should be noted that there is no clear dependence of the column detection limit for long paths. This is different for the 270 m long paths, where the column detection limits are smaller:  $324 \text{ ppb} \times \text{m}$  for benzene,  $345 \text{ ppb} \times \text{m}$  for toluene,  $300 \text{ ppb} \times \text{m}$  for m-xylene, and  $205 \text{ ppb} \times \text{m}$  for p-xylene. The higher column detection limits on longer paths are caused by photon noise, i.e. limitations of the amount of light collected by the system. On the other hand, the 270 m detection limit likely has components of an inaccurate description of the oxygen and ozone absorption.

It should be pointed out that these detection limits are determined from realistic atmospheric measurements, in contrast to those reported for commercial instruments, which are often based on calculation using anticipated noise levels or zero-span drift tests

(Kim, 2004), and thus do not consider the challenges in the analysis of real atmospheric data. In addition, a relative analysis using an atmospheric spectrum generally improves the precision of the analysis at the price of an unknown bias. It is thus not surprising that the detection limits for our absolute measurements are in the same range as those reported by the manufacturers of these instruments. Our detection limits are somewhat better than those from other research grade instruments (see for example Jobson et al. (2010)).

### 3.1. Other measurements

During our field deployment in Houston a number of other measurements were available. Here we will focus on those that can be directly compared to our observation, i.e. meteorological parameters, ozone, benzene, and toluene.

#### 3.1.1. Proton-transfer mass spectrometer

The University of Houston Proton-Transfer Mass Spectrometer (PTRMS) was deployed at the Manchester St. Site, at the location of the LP-DOAS system. During the first five days of the Houston deployment the PTRMS sampled at 15 m altitude, the height of the LP-DOAS telescope. For the rest of the experiment, measurements were performed at 3 m above the ground. The PTRMS measures a suite of hydrocarbons, including benzene, toluene, and the sum of ethyl benzene and the xylenes (Lindinger and Jordan, 1998). The PTRMS was calibrated for select VOC species six times during the month of February using a gas standard provided by Aerodyne and/or HARC. The calibrations consisted of a standard addition of the calibration gas, diluted by flow of zero air at a rate that results in an overflow when the PTRMS samples from line. During the calibrations, the respective PTRMS units operated by Aerodyne and/or HARC were calibrated sampling from the same standard dilution flow. The detection limit for a 1 Hz sampling frequency was 0.92 ppb for benzene, 0.86 ppb for toluene, and 0.83 ppb for the C2-benzenes. While the instrument measures at a 1 Hz frequency, we will use 1-min averaged data in the rest of this manuscript.

#### 3.1.2. Ozone UV absorption

A 2B-Tech dual cell UV absorption ozone instrument was also operated by UH at the Manchester St. site. This instrument sampled at 3 m altitude for the entire experiment in Houston. Ozone mixing ratios have an accuracy of  $\sim 1.5$  ppb.

#### 3.1.3. Meteorological data

Meteorological data was measured by a meteorological station operated by the Texas Commission of Environmental Quality, located on Manchester St. about 500 m from the aforementioned LP-DOAS site (CAMS 1029, [http://www.tceq.state.tx.us/cgi-bin/compliance/monops/site\\_info.pl](http://www.tceq.state.tx.us/cgi-bin/compliance/monops/site_info.pl)).

## 4. Results

The new instrument was used during two field deployments: for 3 months as a fence-line monitor behind a refinery in Los Angeles, and, together with a second, identical instrument in Houston, Texas to measure 2D concentration fields of benzene, toluene and xylenes. We will present the results of the two deployments in this section, after discussing the performance of the new instrument and the new LED light source.

### 4.1. Performance of LED light source

The most innovative aspect of the new instrument is the new dual deep-UV LED light source. It is thus useful to provide

information on its performance during the Houston field experiment. We chose this deployment over the fence-line monitoring experiment as the conditions were much more challenging, thus amplifying any possible problems with the light source. The instrument was operated continuously during a three week period in Houston, except for a few short power failures and a three-day break due to heavy thunderstorms. The light source was located in an aluminum crate outdoors, together with the spectrometer/detector and other electronics. The box was not thermally stabilized and the temperature in the crate changed between 10 and 40 °C. During normal instrument operation, regular observations of the LED signal were made by rotating a diffuse reflective target in front of the bifurcated fiber. It was found that the reflectivity of this target decreased throughout the experiment, and that absolute measurements of light intensity were not possible. The intensities during the atmospheric measurements did not decrease noticeably (not shown), taking into account the high variability of this quantity due to atmospheric effects.

For DOAS applications the stability of the absolute intensity is less important than the spectral stability, which in our case is controlled by the stability of the two LEDs relative to each other. The ratio of the intensities at the two peak wavelengths of the LEDs in the light source spectra showed a variability of up to 10% over the duration of the experiment (Fig. 5). However, the relative intensities vary less over shorter time periods and the changes are fairly smooth, indicating a slow drift rather than random effects. We attribute these drifts to changes in temperature or other environmental conditions in the instrument crate. The fast changes, for example on 2/17 and 2/19, are due to rapid temperature changes when the crate was opened to work on the instrument. However, such changes were corrected in the analysis, as the instrument measured an LED spectrum after each re-start of the normal measurement routine. The insert in Fig. 5 shows the ratio of two LED spectra at the beginning and in the middle of the experiment. The ratio shows a broad spectral structure due to variations in the LED emissions of 2% peak-to-peak. The structure is sufficiently broad that it can easily be removed by the polynomial included in our retrieval fit. Nevertheless, we concluded from our experience in Houston that thermally stabilizing the light source should increase its stability, especially in uncontrolled environments. In addition,

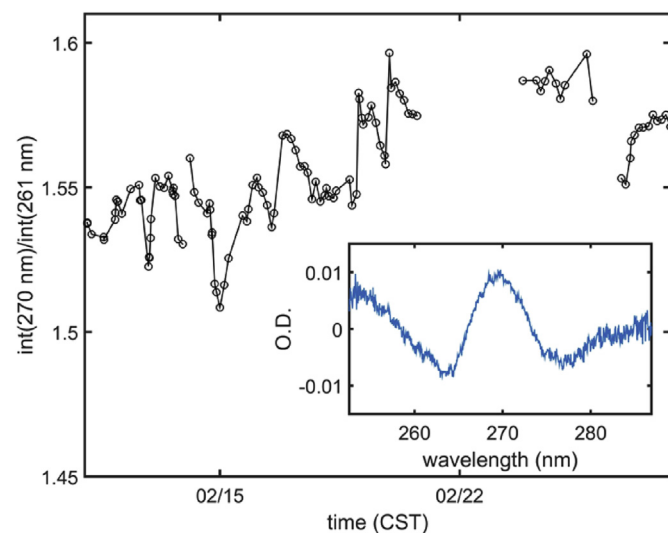


Fig. 5. Ratio of the peak intensities of the two LEDs at 270 nm and 261 nm (see Fig. 2) during the Houston deployment. The insert shows the ratio of LED spectra measured at the beginning and the middle of the experiment.

the measurement of regular LED spectra and the use of these spectra in the analysis will reduce the effect of temperature drifts.

#### 4.2. Toluene and benzene intercomparisons

As part of the Houston experiment we also performed an intercomparison with the PTRMS instrument of the University of Houston. The PTRMS instrument is an in-situ instrument, and care has to be taken when comparing its observations with those from a path-averaging LP-DOAS instrument. To alleviate this problem, the intercomparison was performed on the shortest, 270 m long, light path with the PTRMS inlet located at one end of the light path, at the same altitude as the light path, i.e. 15 m.

A plume of up to 25 ppb of toluene was observed by both instruments on 2/10/15 (Fig. 6). The comparison of the two observations shows excellent agreement, both in the temporal behavior as well as the absolute levels of observed toluene. The red shaded band shows the statistical error of the LP-DOAS observations (see Section 3), which is in the same range as the short-term (1-min) variability of the PTRMS data. A correlation of the PTRMS data integrated over the measurement interval of the LP-DOAS yields: Toluene (LP-DOAS) =  $(1.16 \pm 0.5) \cdot \text{Toluene (PTRMS)} - (1.1 \pm 0.3)$  ppb. It should be noted that this was the only toluene plume that was observed during the 5-day long intercomparison period, and that most of the time both instruments measured mixing ratios close to or below their respective detection limits.

The intercomparison of benzene was considerably more challenging, as the few observed plumes were highly inhomogeneous. As illustrated in Fig. 7, the PTRMS sees highly variable mixing ratios of up to 100 ppb (max values not shown), while the LP-DOAS measures a maximum of 45 ppb benzene at the mid-point of the high PTRMS peaks. We believe that we observed emissions from a railcar parked within ~20–30 m of the PTRMS instrument and that the PTRMS observed individual air parcels from the railcar, while the LP-DOAS provided an average over these air masses. Considering this inhomogeneity, the qualitative agreement between the two observations is quite good. A somewhat more homogeneous, but less concentrated plume on 2/9 is shown in Fig. S3. Here the agreement between the systems is much better, especially during

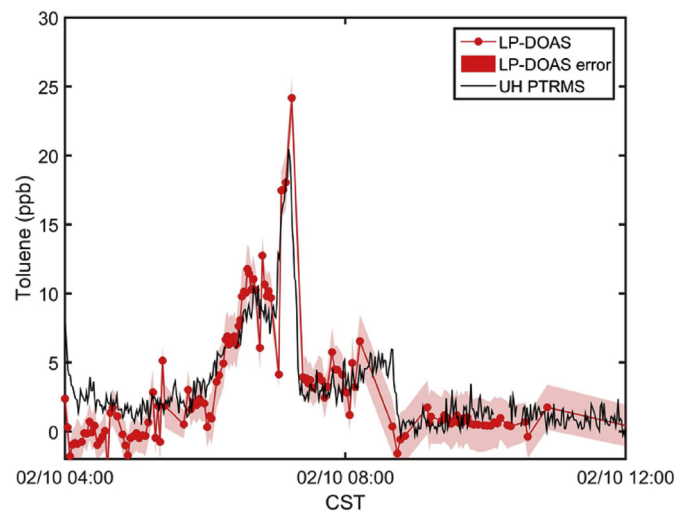


**Fig. 6.** Intercomparison of the LP-DOAS, measuring on a 270 m absorption path, with PTRMS observations during an event with elevated toluene mixing ratios. The shaded area shows the uncertainty of the LP-DOAS measurements. PTRMS data were averaged to 1-min time intervals.

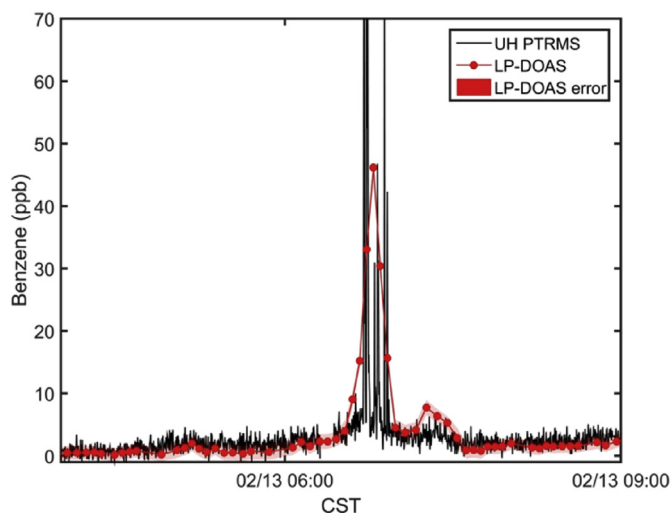


**Fig. 7.** Intercomparison of the LP-DOAS, measuring on a 270 m absorption path, with PTRMS observations during an event with elevated and highly variable benzene mixing ratios. The shaded area shows the uncertainty of the LP-DOAS measurements. PTRMS data were averaged to 1-min time intervals.

the second half of the plume encounter. However, there still appear to be differences that can be attributed to inhomogeneous mixing, which are also apparent in the ozone data. It should also be noted that the plume mixing ratios are quite small, with the LP-DOAS values not exceeding 5 ppb. The figure also shows the very good agreement between the LP-DOAS ozone derived in the benzene analysis window, with the in-situ ozone monitor operated by UH. We are not showing an intercomparison of m- and p-xylene, as the PTRMS only measures the sum of ethyl benzene and the xylenes and the LP-DOAS was not able to detect o-xylene.

Overall, the agreement between the PTRMS and the LP-DOAS is very good, based on the few plumes with mixing ratios above 1–2 ppb we encountered, and the clear challenges of comparing in-situ with path-averaging measurements when measuring close to sources.

#### 4.3. LP-DOAS as fence-line monitor

The initial application for which the new LP-DOAS instrument was designed was long-term fence-line monitoring of benzene, toluene and xylenes. We therefore operated the instrument during a three month period from June to August 2014 on a 230 m long path running parallel to the fence-line of a refinery in Carson, CA. The LP-DOAS was run in automatic mode, with a 1 min time resolution. The instrument operated flawlessly, except for three power failures. A 10 day excerpt of the benzene data set illustrates the performance of the instrument (Fig. 8). Benzene mixing ratios were typically around 0–1 ppb when the LP-DOAS was upwind of the refinery (wind-direction  $\sim 300^\circ$ ), and 2–4 ppb when the LP-DOAS was downwind of the refinery (wind-direction  $90\text{--}270^\circ$ ). We attribute the variability in the up-wind benzene data to the statistical error in our analysis, which is  $\sim 0.5$  ppb during this measurement period. We conclude from this testing period that the new LP-DOAS can be operated with minimal human interaction at sensitivities suitable to measure fugitive emissions from petrochemical facilities at mixing ratios above 0.5–1 ppb. The stability of the new light source and the telescope setup allow long term fully automated operation, providing considerable cost-savings in its operation.

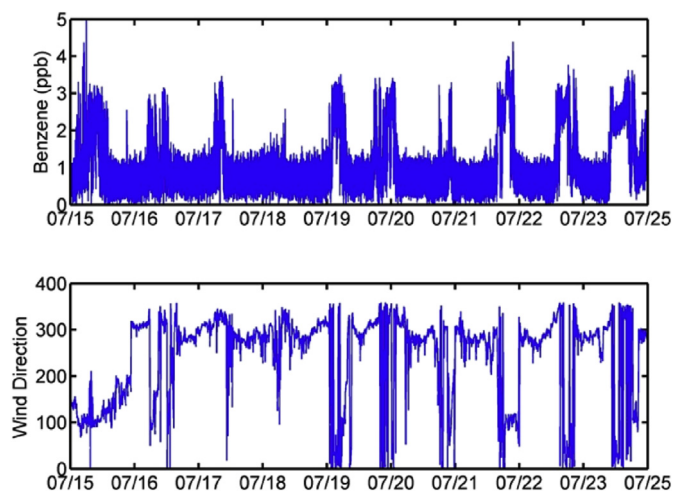


**Fig. 8.** Example of fence-line benzene measurements in Carson, CA. Benzene mixing ratios when air passing over the refinery is sampled (wind direction  $\sim 100^\circ$ ) are about 2 ppb higher than background mixing ratios.

#### 4.4. Observation of 2D concentration distributions

A novel application for aromatics measurements with LP-DOAS is the determination of two-dimensional distributions of benzene, toluene and xylenes using two LP-DOAS instruments with multiple crossed light paths. Such measurements have been reported for  $\text{NO}_2$  (Hartl et al., 2006; Laepple et al., 2004) using LP-DOAS, and ammonia using open-path Fourier Transfer IR Spectroscopy (Todd et al., 2001). However, to our knowledge this has not yet been attempted for aromatic hydrocarbons. The following section will describe the setup of such a LP-DOAS network, discuss the observational data, and present an example of the retrieval results. Details of the retrievals of the 2D mixing ratio fields and the final results are given in a companion paper by Olaguer et al.

Observations were performed during the BEE-TEX field experiment in February 2015 in the Manchester neighborhood in Houston, TX. Two LP-DOAS systems, identical except for the spectrometers, were used. The second instrument used an Acton Spectra Pro 500, and thus had a slightly different spectral resolution and spectral range than the system described in Section 2. However, the data analysis was performed using the same parameters as given in Section 2 (Table 2), and the detection limits were generally comparable.

The setup of the LP-DOAS network is shown in Fig. 9, with details listed in Table 3. One instrument was located at the corner of Manchester St., and 97th St. (Manchester St. Site). The second instrument was located in the northeastern corner of Hartman Park (Hartman Park site). Seven light paths with lengths between 270 and 1203 m were set up (Fig. 9). The Hartman Park instrument cycled between four light paths (H1 – H4), while the Manchester St. instrument measured sequentially on three light paths (M1 – M3). Measurement time on each light path was  $\sim 5$  min. The total time for a full 2D scan, including telescope movement and alignment, was thus  $\sim 25$  min.

High trees in the neighborhood made the setup of the network extremely challenging. Seven retroreflector arrays were set up. The three southern reflectors were mounted on telescopic radio towers at an altitude of 15–20 m above ground level (agl). The two arrays on the western site of the network were mounted on the rail of the IH610 bridge, which crosses the Houston Ship Channel, at altitudes of 20–30 m agl. The last reflector was mounted on the top of the Hartman Park scaffolding tower at 15 m agl. The LP-DOAS systems

were mounted on 15 m high scaffolding towers, which made operation difficult and led to problems when high winds led to movement of the towers, causing a loss of aim onto the reflectors. In addition, the electrical power was sporadic at Hartman Park. Consequently, the dataset has multiple gaps during the measurement period of 2/9/15–2/28/15 for the Manchester Park system and 2/15/15–2/28/15 for the Hartman Park instrument. Nevertheless, both instruments worked simultaneously during extended periods of time, thus allowing the demonstration of the 2D mapping capability of such a setup. It should be noted that the original set-up of the network had two more paths in the southern part of the domain, which were blocked by very high trees and therefore could not be used. However, as will be shown below and explained in more detail in Olaguer et al., the reconstruction of the 2D concentration fields was possible with the 7 absorption paths described here.

During most of the experiment, mixing ratios of aromatics were at or below 1 ppb, near the detection limit of the LP-DOAS instruments. Simultaneous measurements performed by various mobile platforms confirmed the generally low background levels of aromatics in Houston. During two nights, 2/18 and 2/19, however, plumes with high mixing ratios of aromatic hydrocarbons were observed during the late night. We will focus on this period here and qualitatively discuss the spatial distribution of toluene and m- and p-xylene. A different example was chosen for benzene, as benzene levels were quite low during this period, indicating a different set of sources for benzene.

As illustrated in Figs. 10 and 11, mixing ratios of toluene and m- and p-xylene were in the low ppb levels before midnight on 2/18. At 01:00 on 2/18 all Hartman Park light paths, as well as M1 and M2, detected elevated toluene and m- and p-xylene. The event shows two distinct plumes, which are separated by one horizontal scan that is close to background levels. The highest mixing ratios of  $\sim 60$  ppb toluene and 10–20 ppb of the xylenes were observed in the first plume on the H2 light path, with somewhat lower levels on the H1 and M1 paths. These three light paths have the highest coverage in the northwestern part of the DOAS network. For the first plume, the H3, H4 and M2 paths also see the plume, but with lower mixing ratios, while M3, which is located in the southwestern corner of the network, does not show elevated toluene. One can thus qualitatively conclude that the plume was located in the northwestern part of the Manchester neighborhood. The second plume on 2/18 shows a somewhat different behavior in that H1, H3, and M2 have similar mixing ratios, and even M3 shows an increase of the mixing ratios. It thus appears that this plume is mostly in the center of the network, extending partly to the southeastern corner. A third plume only seems to be present in the Manchester St. light paths.

Another event was observed during the following night (Figs. 10 and 11). The behavior of this plume is similar to the one we just described, with the highest mixing ratios on the H1 and H2 paths. However, in this case, the M1 – M3 paths showed little enhancement in mixing ratios, indicating that this plume was limited to the western part of the network. However, the similarity in distribution on the Hartman Park paths seems to point to a common source for the plumes on 2/18 and 2/19. The 2/19 event will be discussed in more detail in Olaguer et al. Surprisingly, the two large toluene/xylene plumes on 2/18 and 2/19 showed little benzene, with a peak benzene mixing ratio on H2 of 6 ppb above a background of 4 ppb on 2/18, and 7 ppb above a background of 4 ppb on 2/19.

The retrieval of 2D trace gas distributions from these observations using the HARC 3D forward and adjoint micro-scale air quality model (Olaguer, 2011) is presented in the companion paper by Olaguer et al. Fig. 12 shows the results for the retrieval of the plume encountered on 2/18/15 at 01:00. The retrieval confirms the



Fig. 9. Setup of the two LP-DOAS instruments and the seven light paths during the BEE-TEX experiment in the Manchester neighborhood in Houston, TX.

**Table 3**  
Retroreflector locations and instrument/reflector distances for the seven absorption paths during the BEE-TEX experiment.

Reflector location	Distance (m)
<b>Manchester St. LP-DOAS</b>	
M1 LP-DOAS scaffolding tower at Hartman Park	770
M2 Southern end of IH610 bridge	1203
M3 Telescopic tower south of LP-DOAS	270
<b>Hartman Park LP-DOAS</b>	
H1 IH610 bridge	513
H2 Southern end of IH610 bridge	526
H3 Telescopic tower at the exit ramp of the IH bridge	689
H4 Telescopic tower near the Central St. bridge	740

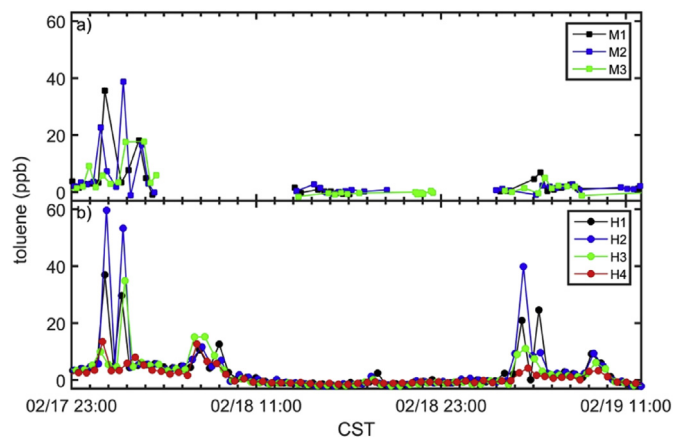


Fig. 10. Toluene on all seven light paths during a period with two nighttime plumes. Panel a) shows the observations from the Manchester St. site, with the data color coded according to light paths. Panel b) shows the four different light paths of the Hartman Park site.

qualitative interpretation of the LP-DOAS observations, by placing the highest toluene mixing ratios and its source in the north-western corner of the Manchester neighborhood. Peak mixing

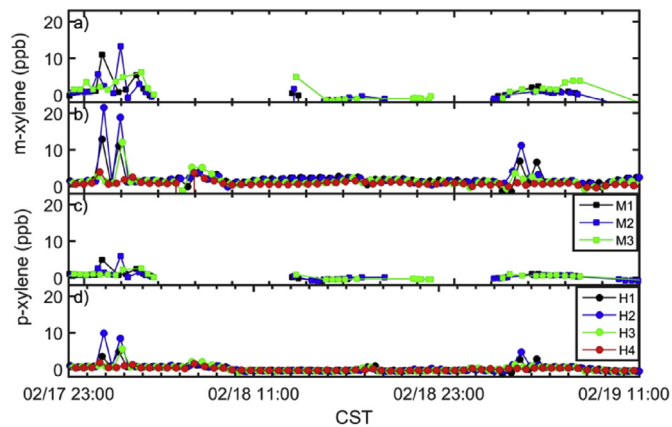
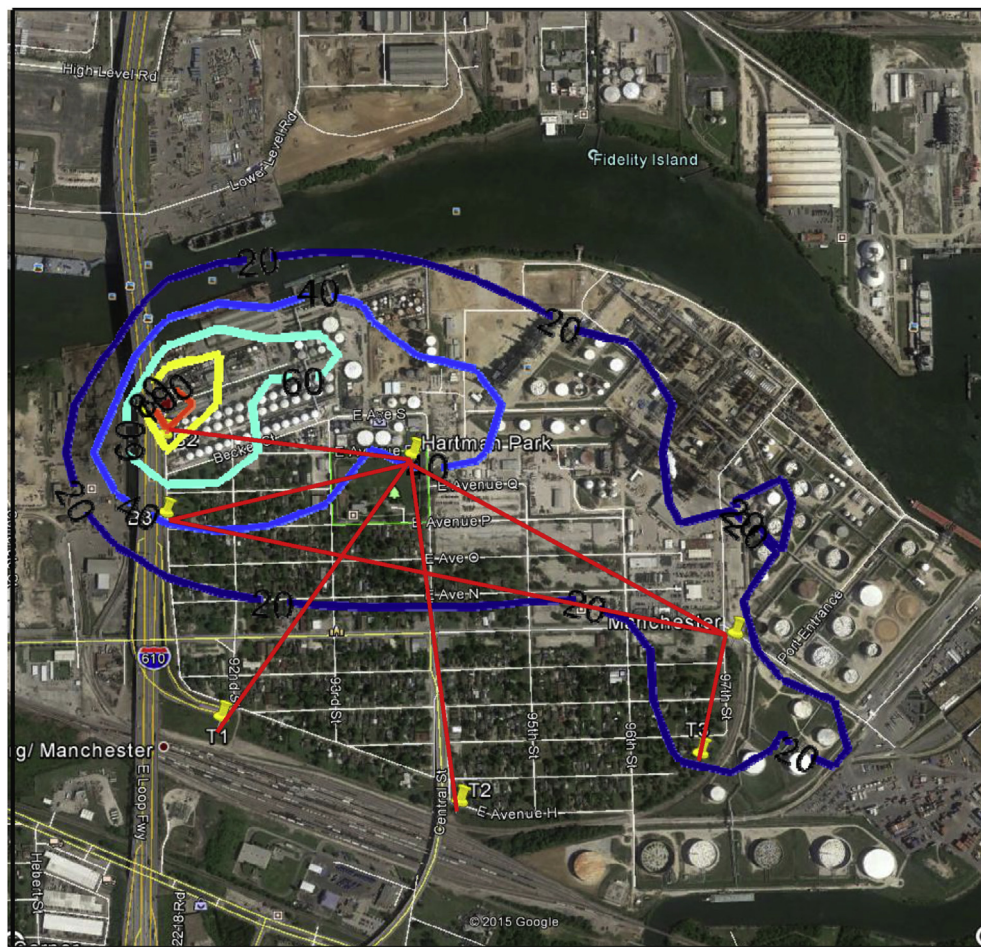


Fig. 11. m-xylene (panels a & b) and p-xylene (panels c & d) on all seven light paths during a period with two nighttime plumes. The observations show the same period as in Fig. 10.

ratios are around 60–80 ppb, higher than those observed by the LP-DOAS. However, the overlaid light paths show that the H1 and H2 LP-DOAS paths also capture the already diluted part of the plume, thus explaining the somewhat lower observed mixing ratios. The lower H3 and H4 mixing ratios can be explained by the fast decrease of the toluene mixing ratios southwards.

**5. Conclusions**

The goal of this study was to demonstrate a novel LP-DOAS system specifically developed for the measurement of aromatic hydrocarbons. Two applications were presented: one LP-DOAS as a long term fence-line monitor, and a dual LP-DOAS network to perform two-dimensional observations of trace gas distributions. The following conclusions can be drawn from our experience with the new LP-DOAS system:



**Fig. 12.** Retrieval of the spatial distribution of toluene in the Manchester Neighborhood in Houston, TX, on 2/18/15 at 01:00. The retrieval is based on the LP-DOAS data shown in Fig. 10 and the HARC model described in the companion manuscript by Olaguer et al. Numbers in the figures are toluene mixing ratios in ppb.

- A new light source, which combines two LEDs using a fiber mixer, is suitable for LP-DOAS observations of aromatic hydrocarbons. The use of LEDs solves the problem of large stray light levels due to light with wavelengths smaller than 290 nm encountered when using Xe-arc lamps. It is also longer lived and more stable than comparable Xe-arc lamps. While we demonstrated this setup in the UV wavelength range, it should also be applicable for DOAS observations in other wavelength ranges by using other LED combinations.
- The new instrument, together with an improved analysis algorithm, allows the absolute determination of BTX concentrations without the use of an atmospheric reference spectrum. This is a significant improvement compared to many commercial systems, which predominately measure relative to this reference spectrum.
- We demonstrated that dedicated LP-DOAS instruments are capable of measuring aromatic hydrocarbons on light paths from 270 to 1200 m length, with detection limits below 1 ppb. Comparison with in-situ data shows very good agreement in cases where a well-mixed plume is encountered. However, close to sources the high variability of the data makes a comparison difficult. To our knowledge this is the first time a BTX LP-DOAS system has successfully been operated on light paths longer than 700 m. This ability expands the possible applications of BTX LP-DOAS.
- The new light source, together with a stable telescope setup and thermally stabilized spectrometers, is capable of performing long-term automated observations of aromatics along the fence-line of a petrochemical facility. The 1 min time resolution, together with a near-real time data analysis (~30 s after measurements) allows this system to also be used as an alarm system for accidental releases from a facility.
- A network composed of two near-identical LP-DOAS instruments measuring on seven crossing light paths is capable of obtaining information on the horizontal distribution of aromatic hydrocarbons. This approach allows the identification of emission sources in near-real time, as demonstrated during BEE-TEX.

Our results demonstrate the potential of LP-DOAS as a powerful tool to monitor air-toxics levels as well as to identify their sources. We demonstrate that systems based on our design can address the monitoring requirements for benzene and other aromatics put forward by the new EPA rule on petrochemical facility emissions (<http://www.epa.gov/airtoxics/petref.html>). The high sensitivity of the new instrument also allows distinguishing of elevated BTX levels near petrochemical facilities, which are typically at or above 1 ppb, from typical ambient levels of below 0.5 ppb, something that has been elusive for commercial LP-DOAS systems. The proposed design, and especially the LED setup, offers opportunities to develop cheaper systems. In particular, the use of less sophisticated

spectrometers could reduce the cost of the instrument considerably. In addition, smaller telescopes can be used if light path lengths do not exceed 500 m. Ultimately, such systems could enable automated continuous monitoring of benzene, toluene, and xylene levels around and inside petrochemical facilities.

## Acknowledgements

We would like to thank Paul Northrop for help in developing and building the new LP-DOAS system. The fence-line monitoring efforts were funded by the South Coast Air Quality Management District. BEE-TEX was funded by the Fish and Wildlife Service of the U.S. Department of the Interior through Harris County, Texas.

## Appendix A. Supplementary data

Supplementary data related to this article can be found at <http://dx.doi.org/10.1016/j.atmosenv.2016.09.054>.

## References

- Axelsson, H., Eilard, A., Emanuelsson, A., Galle, B., Edner, H., Ragnarson, P., Kloo, H., 1995. Measurement of aromatic hydrocarbons with the DOAS technique. *Appl. Spectrosc.* 49, 1254–1260. <http://dx.doi.org/10.1366/0003702953965254>.
- Barrefors, G., 1996. Monitoring of benzene, toluene and p-xylene in urban air with differential optical absorption spectroscopy technique. *Sci. Total Environ.* 189–190, 287–292. [http://dx.doi.org/10.1016/0048-9697\(96\)05221-7](http://dx.doi.org/10.1016/0048-9697(96)05221-7).
- Fally, S., Carleer, M., Vandaele, A.C., 2009. UV Fourier transform absorption cross sections of benzene, toluene, meta-, ortho-, and para-xylene. *J. Quant. Spectrosc. Radiat. Transf.* 110, 766–782. <http://dx.doi.org/10.1016/j.jqsrt.2008.11.014>.
- Fally, S., Vandaele, A., Carleer, M., Hermans, C., Jenouvrier, A., Mérienne, M., Coquart, B., Colin, R., 2000. Fourier transform spectroscopy of the O(2) Herzberg bands. III. Absorption cross sections of the collision-induced bands and of the Herzberg continuum. *J. Mol. Spectrosc.* 204, 10–20. <http://dx.doi.org/10.1006/jmsp.2000.8204>.
- Finlayson-Pitts, B.J., Pitts, J.N., 1999. *Chemistry of the Upper and Lower Atmosphere: Theory, Experiments, and Applications*. Academic Press. <http://dx.doi.org/10.1016/B978-0-12-257060-5.50027-7>.
- Hartl, A., Song, B.C., Pundt, I., 2006. 2-D reconstruction of atmospheric concentration peaks from horizontal long path DOAS tomographic measurements: parametrisation and geometry within a discrete approach. *Atmos. Chem. Phys.* 6, 847–861. <http://dx.doi.org/10.5194/acp-6-847-2006>.
- Jobson, B.T., Volkamer, R.A., Velasco, E., Allwine, G., Westberg, H., Lamb, B.K., Alexander, M.L., Berkowitz, C.M., Molina, L.T., 2010. Comparison of aromatic hydrocarbon measurements made by PTR-MS, DOAS and GC-FID during the MCMA 2003 Field Experiment. *Atmos. Chem. Phys.* 10, 1989–2005. <http://dx.doi.org/10.5194/acp-10-1989-2010>.
- Kim, K., Kim, M., 2001. Comparison of an open path differential optical absorption spectroscopy system and a conventional in situ monitoring system on the basis of long-term measurements of SO<sub>2</sub>, NO<sub>2</sub>, and O<sub>3</sub>. *Atmos. Environ.* 35, 4059–4072. [http://dx.doi.org/10.1016/S1352-2310\(01\)00216-3](http://dx.doi.org/10.1016/S1352-2310(01)00216-3).
- Kim, K.-H., 2004. Comparison of BTX measurements using a differential optical absorption spectroscopy and an on-line gas chromatography system. *Environ. Eng. Sci.* 21, 181–194. <http://dx.doi.org/10.1089/109287504773087354>.
- Laepple, T., Knab, V., Mettendorf, K.-U., Pundt, I., 2004. Longpath DOAS tomography on a motorway exhaust gas plume: numerical studies and application to data from the BAB II campaign. *Atmos. Chem. Phys. Discuss.* 4, 2435–2484. <http://dx.doi.org/10.5194/acpd-4-2435-2004>.
- Lee, C., Choi, Y., Jung, J., Lee, J., Kim, K., Kim, Y., 2005. Measurement of atmospheric monoaromatic hydrocarbons using differential optical absorption spectroscopy: comparison with on-line gas chromatography measurements in urban air. *Atmos. Environ.* 39, 2225–2234. <http://dx.doi.org/10.1016/j.atmosenv.2005.01.004>.
- Lindinger, W., Jordan, A., 1998. Proton-transfer-reaction mass spectrometry (PTR-MS): on-line monitoring of volatile organic compounds at pptv levels. *Chem. Soc. Rev.* 27, 347–375. <http://dx.doi.org/10.1039/a827347z>.
- Merten, A., Tschirner, J., Platt, U., 2011. Design of differential optical absorption spectroscopy long-path telescopes based on fiber optics. *Appl. Opt.* 50, 738–754. <http://dx.doi.org/10.1364/AO.50.000738>.
- Olague, E.P., 2011. Adjoint model enhanced plume reconstruction from tomographic remote sensing measurements. *Atmos. Environ.* 45, 6980–6986. <http://dx.doi.org/10.1016/j.atmosenv.2011.09.020>.
- Peng, F., Xie, P., Li, H., Zhang, Y., Wang, J., Liu, W., 2008. Effect of atmospheric interfering absorption on measurement of BTX by DOAS. *Chin. J. Chem. Phys.* 21, 202–210. <http://dx.doi.org/10.1088/1674-0068/21/03/202-210>.
- Platt, U., Stutz, J., 2008. *Differential Optical Absorption Spectroscopy, Physics of Earth and Space Environments*. Springer-Verlag, Berlin Heidelberg. <http://dx.doi.org/10.1007/978-3-540-75776-4>.
- Sihler, H., Kern, C., Pöhler, D., Platt, U., 2009. Applying light-emitting diodes with narrowband emission features in differential spectroscopy. *Opt. Lett.* 34, 3716–3718.
- Skov, H., 2001. An overview of commonly used methods for measuring benzene in ambient air. *Atmos. Environ.* 35, 141–148. [http://dx.doi.org/10.1016/S1352-2310\(00\)00512-4](http://dx.doi.org/10.1016/S1352-2310(00)00512-4).
- Snyder, R., Witz, G., Goldstein, B.D., 1993. The toxicology of benzene. *Environ. Health Perspect.* 100, 293–306.
- Stutz, J., Platt, U., 1997. Improving long-path differential optical absorption spectroscopy with a quartz-fiber mode mixer. *Appl. Opt.* 36. <http://dx.doi.org/10.1364/AO.36.001105>.
- Todd, L.A., Ramanathan, M., Mottus, K., Katz, R., Dodson, A., Mihlan, G., 2001. Measuring chemical emissions using open-path Fourier transform infrared (OP-FTIR) spectroscopy and computer-assisted tomography. *Atmos. Environ.* 35, 1937–1947. [http://dx.doi.org/10.1016/S1352-2310\(00\)00546-X](http://dx.doi.org/10.1016/S1352-2310(00)00546-X).
- Trost, B., Stutz, J., Platt, U., 1997. UV-absorption cross sections of a series of monocyclic aromatic compounds. *Atmos. Environ.* 31, 3999–4008. [http://dx.doi.org/10.1016/S1352-2310\(97\)00214-8](http://dx.doi.org/10.1016/S1352-2310(97)00214-8).
- Villanueva, F., Notario, A., Mabilia, R., Albaladejo, J., Cabañas, B., Martínez, E., 2012. Intercomparison of tropospheric O<sub>3</sub>, benzene and toluene measured by a commercial DOAS system and conventional monitoring techniques. *Fresenius Environ. Bull.* 21, 4040–4050.
- Voigt, S., Orphal, J., Bogumil, K., Burrows, J.P., 2001. The temperature dependence (203–293 K) of the absorption cross sections of O<sub>3</sub> in the 230–850 nm region measured by Fourier-transform spectroscopy. *J. Photochem. Photobiol. A Chem.* 143, 1–9. [http://dx.doi.org/10.1016/S1010-6030\(01\)00480-4](http://dx.doi.org/10.1016/S1010-6030(01)00480-4).
- Volkamer, R., Etkorn, T., Geyer, A., Platt, U., 1998. Correction of the oxygen interference with UV spectroscopic (DOAS) measurements of monocyclic aromatic hydrocarbons in the atmosphere. *Atmos. Environ.* 32, 3731–3747. [http://dx.doi.org/10.1016/S1352-2310\(98\)00095-8](http://dx.doi.org/10.1016/S1352-2310(98)00095-8).
- Weisel, C.P., 2010. Benzene exposure: an overview of monitoring methods and their findings. *Chem. Biol. Interact.* 184, 58–66. <http://dx.doi.org/10.1016/j.cbi.2009.12.030>.
- Wideqvist, U., Vesely, V., Johansson, C., Potter, A., Brorström-Lundén, E., Sjöberg, K., Jonsson, T., 2003. Comparison of measurement methods for benzene and toluene. *Atmos. Environ.* 37, 1963–1973. [http://dx.doi.org/10.1016/S1352-2310\(03\)00029-3](http://dx.doi.org/10.1016/S1352-2310(03)00029-3).
- Xie, P., Liu, W., Fu, Q., Wang, R., Liu, J., Wei, Q., 2004. Intercomparison of NO<sub>x</sub>, SO<sub>2</sub>, O<sub>3</sub>, and aromatic hydrocarbons measured by a commercial DOAS system and traditional point monitoring techniques. *Adv. Atmos. Sci.* 21, 211–219. <http://dx.doi.org/10.1007/BF02915707>.